Journal of Computational Science and Technology

Vol. 3, No. 1, 2009

Stress Intensity Factor for a Rectangular Interface Crack in Three Dimensional Bimaterials*

Nao-Aki NODA**, Chunhui XU*** and Yasushi TAKASE****
** Department of Mechanical Engineering, Kyushu Institute of Technology
Sensui-Cho 1-1 Tobata-Ku, Kitakyushu-Shi, Fukuoka, Japan
E-mail: noda@mech.kyutech.ac.jp
***College of Science, China Agricultural University, Beijing 100083, P.R.CHINA
E-mail:xuchunhui_cau@163.com
**** Department of mechanical Engineering, Kyushu Institute of Technology
Sensui-Cho 1-1 Tobata-Ku, Kitakyushu-Shi, Fukuoka, Japan
E-mail: takase@mech.kyutech.ac.jp

Abstract
In this paper, stress intensity factors for a three dimensional rectangular interfacial crack are considered on the idea of the body force method. In the numerical calculations, unknown body force densities are approximated by the products of the fundamental densities and power series; here the fundamental densities are chosen to express singular stress fields due to an interface crack exactly. The calculation shows that the present method gives rapidly converging numerical solutions and highly satisfied boundary conditions. The stress intensity factors for a rectangular interface crack are indicated accurately with varying the aspect ratio, and biomaterial parameter.

Key words: Elasticity, Stress Intensity Factor, Body Force Method, Interface Crack, Fracture Mechanics, Composite Material, Singular Integral Equation

1. Introduction

In recent years, composite materials and adhesive or bonded joints are widely used in many fields especially for electronic products. Failures of those products are dominated by interfacial destruction because they usually originate from the interfacial region. From this aspect, the accurate evaluation of interface cracks in dissimilar materials has been important. For interfacial cracks, a number of analyses [1]-[18] have been made; however, usually they are limited under specific material combinations. Closed form solutions for stress intensity factors (SIFs) are available only for penny-shaped interfacial crack [17], deep external interfacial crack[18], and ring-shaped interfacial crack[19] under any combinations of materials. Usually, considering the oscillation singularity and overlapping of crack surfaces around the crack tip is difficult although both of them are peculiar to interface cracks.

In our previous paper [20], accurate numerical solutions were considered for 3D interfacial crack problems on the basis of hypersingular intergro-differential equations derived by Chen-Noda-Tang[21] considering the oscillation singularity and overlapping of crack surfaces. The proposed method may be useful for expressing singular behavior and providing smooth distributions stress intensity factors along crack front with highly satisfied boundary. Therefore, in this paper, a 3D interfacial rectangular crack will be analyzed and the effect of material combination and geometrical conditions on the stress intensity factors will be discussed with varying the material combinations and geometrical conditions.

*Received 19 Dec., 2008 (No. T1-06-1027)
Japanese Original : Trans. Jpn. Soc. Mech. Eng., Vol.73, No.728, A (2007), pp.468-474 (Received 16 Oct., 2006)
[DOI: 10.1299/jcst.3.224]

2. Singular intergro-differential equations for 3D biomaterial interfacial crack problems

Consider two dissimilar elastic half-spaces bonded together along the $x-y$ plane subjected to stresses $\sigma_z^\infty = \sigma_0, \tau_{yz}^\infty = 0, \tau_{zx}^\infty = 0$ at the infinity as shown in Fig.1. There is a rectangular interface crack whose length and width are 2a and 2b respectively. Here μ_1, μ_2 are shear modulus, ν_1, ν_2 are Poisson ratios of the materials. The problem is formulated as a system of hypersingular intergro-differential equations (1) derived by Chen-Noda-Tang [21].

$$\mu_1(\Lambda_2-\Lambda_1)\frac{\partial \Delta u_z(x,y)}{\partial x}+\mu_1\frac{(2\Lambda-\Lambda_1-\Lambda_2)}{2\pi}\fint_s \frac{1}{r^3}\Delta u_x(\xi,\eta)dS(\xi,\eta)$$
$$+3\mu_1\frac{(\Lambda_1+\Lambda_2-\Lambda)}{2\pi}\left\{\fint_s \frac{(x-\xi)^2}{r^5}\Delta u_x(\xi,\eta)dS(\xi,\eta)+\fint_s \frac{(x-\xi)(y-\eta)}{r^5}\Delta u_y(\xi,\eta)dS(\xi,\eta)\right\}=-p_x(x,y) \quad (1a)$$

$$\mu_1(\Lambda_2-\Lambda_1)\frac{\partial \Delta u_z(x,y)}{\partial y}+\mu_1\frac{(2\Lambda-\Lambda_1-\Lambda_2)}{2\pi}\fint_s \frac{1}{r^3}\Delta u_y(\xi,\eta)dS(\xi,\eta)$$
$$+3\mu_1\frac{(\Lambda_1+\Lambda_2-\Lambda)}{2\pi}\left\{\fint_s \frac{(x-\xi)(y-\eta)}{r^5}\Delta u_x(\xi,\eta)dS(\xi,\eta)+\fint_s \frac{(y-\eta)^2}{r^5}\Delta u_y(\xi,\eta)dS(\xi,\eta)\right\}=-p_y(x,y) \quad (1b)$$

$$\mu_1(\Lambda_1-\Lambda_2)\left(\frac{\partial \Delta u_x(x,y)}{\partial x}+\frac{\partial \Delta u_y(x,y)}{\partial y}\right)+\mu_1\frac{(\Lambda_1+\Lambda_2)}{2\pi}\fint_s \frac{1}{r^3}\Delta u_z(\xi,\eta)dS(\xi,\eta)=-p_z(x,y) \quad (1c)$$

$$\Delta u_i(x,y)=u_i(x,y,0^+)-u_i(x,y,0^-),\ (i=x,y,z) \quad (1d)$$

$$\Lambda=\frac{\mu_2}{\mu_1+\mu_2},\quad \Lambda_1=\frac{\mu_2}{\mu_1+\kappa_1\mu_2},\quad \Lambda_2=\frac{\mu_2}{\mu_2+\kappa_2\mu_1},$$
$$\kappa_1=3-4\nu_1,\quad \kappa_2=3-4\nu_2,\quad r^2=(x-\xi)^2+(y-\eta)^2 \quad (1e)$$

Here, $\Delta u_i(x,y)$ means unknown crack opening displacement on the interface in the i direction. The integrals including in Eq. (1) should be interpreted in a sense of finite part integrals.

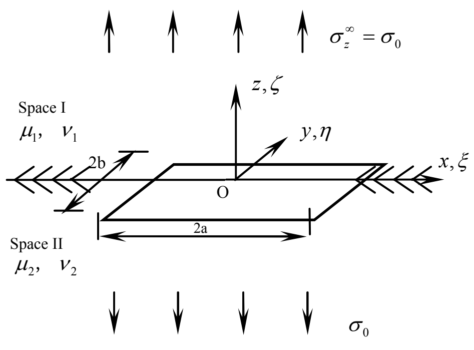

Fig.1 Problem configuration

3. Outline of the method of analysis

In this paper the outline of the method of analysis will be indicated since the details were described in the previous paper [20]. In solving ordinary crack problems the unknown densities were accurately obtained by using the fundamental densities, which express exact solutions for 2D cracks. For interfacial cracks, available solutions are indicated in Figure 2 for a 2D interface crack with a length of 2a under normal stress σ_0 and shear stress τ_0 at the infinity. Crack opening displacements for Fig.2 $\Delta u_x, \Delta u_y, \Delta u_z$ in relation to fundamental density functions $w_x(\xi), w_y(\xi), w_z(\xi)$ can be expressed in the following equations [4].

For Fig. 2(a):

$$\Delta u_z + i\Delta u_x = \sum_{l=1}^{2}\left\{\frac{\kappa_l - 1}{\mu_l(1+\kappa_l)} w_x(\xi) + i\frac{1}{\mu_l} w_y(\xi)\right\} \times (\sigma_0 + i\tau_0)$$

$$= \sum_{l=1}^{2} \frac{1+\kappa_l}{\mu_l 4\cosh \pi\varepsilon}\sqrt{a^2-\xi^2}\left(\frac{a-\xi}{a+\xi}\right)^{i\varepsilon} \tag{2}$$

For Fig. 2(b):

$$\Delta u_y = \sum_{l=1}^{2}\frac{1}{\mu_l} w_y(\xi)\tau_0 = \sum_{l=1}^{2}\frac{1}{\mu_l}\frac{1+\kappa_l}{4}\sqrt{c^2-\xi^2}\,\tau_0 \tag{3}$$

Here, σ_0, τ_0 are the tensile stress and shear stress applied at infinity, and ε and κ are defined as follows.

$$\varepsilon = \frac{1}{2\pi}\ln\left(\frac{\mu_2\kappa_1+\mu_1}{\mu_1\kappa_2+\mu_2}\right), \quad \kappa_l = \begin{cases} \dfrac{3-v_l}{1+v_l} & \text{plane stress} \\ 3-4v_l & \text{plane strain} \end{cases} \tag{4}$$

In present paper, we assume the following expression.

$$\Delta u_i\left(\xi,\eta\right) = w_i(\xi,\eta)F_i(\xi,\eta), \quad i = x, y, z \tag{5}$$

Here, fundamental densities $w_i(\xi,\eta)$, which express oscillation singularity of interface cracks, are defined as follows.

$$w_x(\xi,\eta) = \sum_{l=1}^{2}\frac{1+\kappa_l}{4\mu_l\cosh\pi\varepsilon}\sqrt{a^2-\xi^2}\sqrt{b^2-\eta^2}\times\sin\left(\varepsilon\ln\left(\frac{a-\xi}{a+\xi}\right)\right), \tag{6a}$$

$$w_y(\xi,\eta) = \sum_{l=1}^{2}\frac{1+\kappa_l}{4\mu_l\cosh\pi\varepsilon}\sqrt{a^2-\xi^2}\sqrt{b^2-\eta^2}\times\sin\left(\varepsilon\ln\left(\frac{b-\eta}{b+\eta}\right)\right), \tag{6b}$$

$$w_z(\xi,\eta) = \sum_{l=1}^{2}\frac{1+\kappa_l}{4\mu_l\cosh\pi\varepsilon}\sqrt{a^2-\xi^2}\sqrt{b^2-\eta^2}\times\cos\left(\varepsilon\ln\left(\frac{a-\xi}{a+\xi}\right)\right)\cos\left(\varepsilon\ln\left(\frac{b-\eta}{b+\eta}\right)\right). \tag{6c}$$

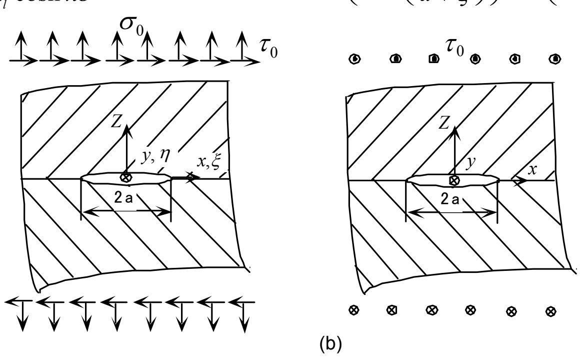

Fig2. Fundamental densities for two dimensional problems

Here the weight functions $F_x(\xi,\eta), F_y(\xi,\eta), F_z(\xi,\eta)$ are approximated by polynomials. As an example, $F_x(\xi,\eta)$ may be expressed in the following equations.

$$F_x(\xi,\eta) = \alpha_0 + \alpha_1\eta + \cdots + \alpha_{n-1}\eta^{(n-1)} + \alpha_n\eta^n + \alpha_{n+1}\xi + \alpha_{n+2}\xi\eta + \cdots + \alpha_{2n}\xi\eta^n + \cdots$$
$$+\alpha_{l-n-1}\xi^m + \alpha_{l-n}\xi^m\eta + \cdots + \alpha_{l-1}\xi^m\eta^n = \sum_{i=0}^{l-1}\alpha_i G_i(\xi,\eta) \quad (7)$$

4. Results and discussion

4.1 The definition of dimensionless stress intensity factors

On the basis of the theory mentioned above, calculations are performed with varying the polynomial exponents m,n in Eq. (7) for a/b=1, 2, 4, 8 and ε=0-0.1. Then, smooth distributions are obtained for the stress intensity factors along the crack front. Here, the normalized stress intensity factors F_{I}, F_{II}, F_{III} as shown in Eq. (8) will be used to indicate the results. The boundary conditions are considered at the 10×10 collocation points imagined on the mesh at the crack surface. The least square regression method is applied to minimize the residual stress to determining the coefficients in the polynomials $\alpha_i, \beta_i, \gamma_i$ in Eq. (7).

$$F_I + iF_{II} = \frac{K_I(x,y)\big|_{x=x,y=\pm b} + iK_{II}(x,y)\big|_{x=x,y=\pm b}}{\sigma_z^\infty\sqrt{\pi b}}$$
$$= \sqrt{a^2 - x^2}\times\left(\cos\left(\varepsilon\ln(\frac{a-x}{a+x})\right)F_z(x,y)\big|_{x=x,y=\pm b} + 2i\varepsilon F_y(x,y)\big|_{x=x,y=\pm b}\right), \quad (8.a)$$

$$F_{III} = \frac{K_{III}(x,y)\big|_{x=x,y=\pm b}}{\sigma_z^\infty\sqrt{\pi a}} = \sum_{l=1}^{2}\frac{1+\kappa_l}{4\mu_l\cosh\pi\varepsilon}\times\frac{1}{(1/\mu_1+1/\mu_2)}\sqrt{a^2-x^2}\sin\left(\varepsilon\ln(\frac{a-x}{a+x})\right)F_x(x,y)\big|_{x=x,y=\pm b}. \quad (8.b)$$

4.2 Convergence of the results

Figure 3(a) - 3(c) shows the compliance of the boundary condition when a/b=1 and $\varepsilon = 0.02$. The remaining stresses $(\sigma_z/\sigma_z^\infty + 1)$, $\tau_{yz}/\sigma_z^\infty$, $\tau_{zx}/\sigma_z^\infty$, which should be zero along the crack surface, are less than 4.4×10^{-5} when $m=n$=6. Those values become smaller than 1.5×10^{-6} when $m=n$=8. The compliance of the boundary conditions is better than the case for the crack terminating at an interface [22] and almost similar to the case of an internal crack in a homogeneous material [23]. It is known that the boundary condition for a surface crack [24] cannot be satisfied very accurately as shown in Fig.3. Usually the boundary conditions for interface cracks are difficult to be satisfied because of the peculiar behavior of oscillation singularity. However, the present method of analysis provides accurate solutions by introducing the fundamental densities and performing numerical integrals with using double exponent integration formula. Table 1 indicates the results for homogeneous material comparing the previous results [22], [23]. As shown in Table 1, the present method shows good convergence for all other cases.

Table1 Convergence of stress intensity factor F_I for ε=0, a/b=1 at $y=b$ (Collocation point 20×20)

x/a	0/11	1/11	2/11	3/11	4/11	5/11	6/11	7/11	8/11	9/11	10/11
m=n=4	0.7521	0.7507	0.7462	0.7379	0.7250	0.7066	0.6821	0.6509	0.6108	0.5538	0.4497
m=n=6	0.7538	0.7520	0.7467	0.7377	0.7248	0.7072	0.6836	0.6520	0.6094	0.5482	0.4423
m=n=8	0.7534	0.7516	0.7463	0.7373	0.7243	0.7063	0.6821	0.6500	0.6081	0.5513	0.4543
Qin	0.7534	0.7512	0.7462	0.7379	0.7255	0.7072	0.6821	0.6497	0.6090	0.5521	0.4464
Wang	0.7534	0.7517	0.7465	0.7376	0.7245	0.7066	0.6828	0.6512	0.6086	0.5492	0.4536

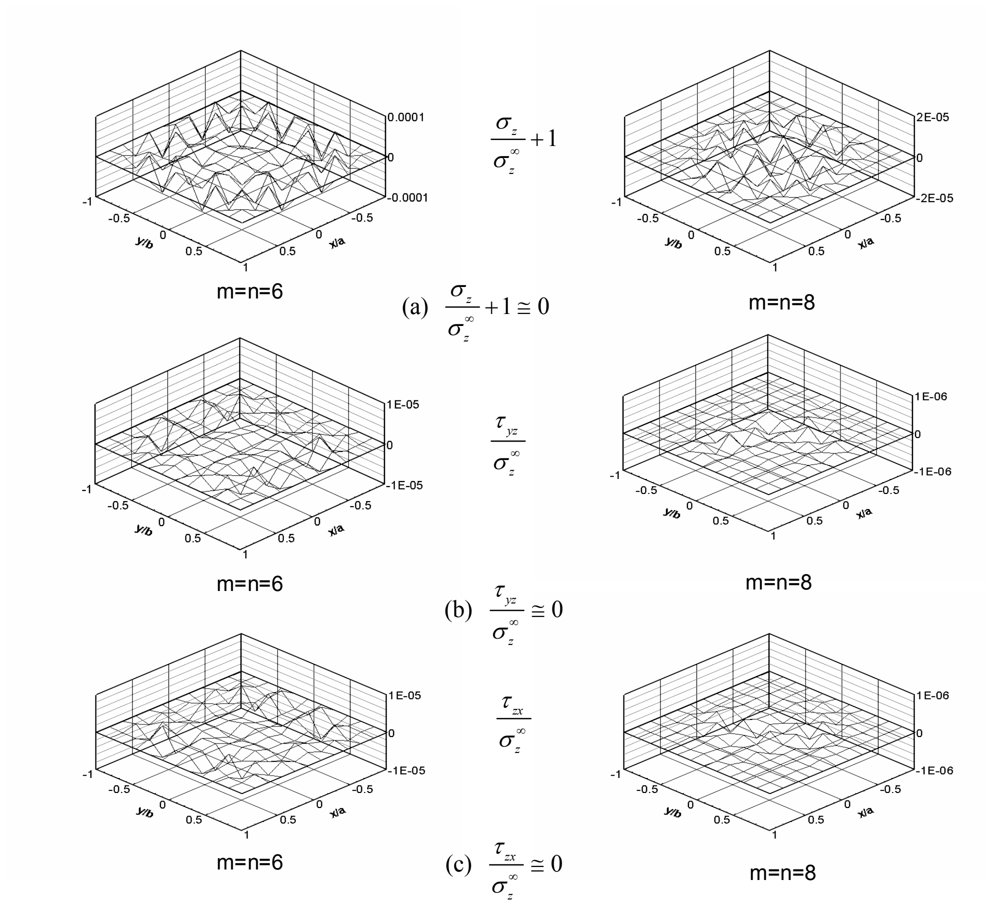

Fig.3 Compliance of boundary condition for $a/b=1,\ \varepsilon=0.02$

4.3 Comparison with the two-dimension case

For large aspect ratio a/b, the results should coincide with the two-dimensional solution. For a/b=8 the stress intensity factors $F_{\mathrm{I}}, F_{\mathrm{II}}, F_{\mathrm{III}}$ shown in Eq. (8) are given in Table 2 when the polynomial exponents $m=n=8$. It is seen that the present results coincide with the two-dimensional exact solution known as $F_I=1, F_{II}=2\varepsilon$, $F_{III}=0$ as $a/b\to\infty$ in the range of $|x/a|\le 0.5$.

Table 2(a) Dimensionless stress intensity factor F_{I} for $a/b=8$ at $y=b$

x/a	0/11	1/11	2/11	3/11	4/11	5/11	6/11	7/11	8/11	9/11	10/11
ε =0.02	0.9947	0.9946	0.9942	0.9933	0.9917	0.9888	0.9838	0.9750	0.9580	0.9175	0.7954
ε =0.04	0.9938	0.9937	0.9932	0.9923	0.9907	0.9878	0.9828	0.9739	0.9568	0.9160	0.7931
ε =0.06	0.9920	0.9919	0.9914	0.9905	0.9889	0.9860	0.9809	0.9719	0.9545	0.9134	0.7892
ε =0.08	0.9891	0.9890	0.9885	0.9875	0.9859	0.9830	0.9779	0.9687	0.9509	0.9092	0.7836
ε =0.10	0.9848	0.9847	0.9842	0.9833	0.9816	0.9786	0.9733	0.9640	0.9461	0.9037	0.7755

Table 2(b) Dimensionless stress intensity factor F_{II} for $a/b=8$ at $y=b$

x/a	0/11	1/11	2/11	3/11	4/11	5/11	6/11	7/11	8/11	9/11	10/11
ε =0.02	0.0397	0.0397	0.0396	0.0396	0.0395	0.0394	0.0391	0.0387	0.0378	0.0358	0.0304
ε =0.04	0.0786	0.0786	0.0785	0.0784	0.0783	0.0780	0.0775	0.0766	0.0749	0.0710	0.0601
ε =0.06	0.1160	0.1160	0.1160	0.1158	0.1156	0.1152	0.1144	0.1131	0.1106	0.1047	0.0885
ε =0.08	0.1515	0.1515	0.1514	0.1512	0.1509	0.1503	0.1493	0.1476	0.1442	0.1364	0.1151
ε =0.10	0.1845	0.1845	0.1844	0.1842	0.1838	0.1831	0.1819	0.1797	0.1755	0.1658	0.1394

Table2(c) Dimensionless stress intensity factor $F_{III} \times 10^{-3}$ for $a/b=8$ at $y=b$ ($\nu_1=\nu_2=0.3$)

x/a	0/11	1/11	2/11	3/11	4/11	5/11	6/11	7/11	8/11	9/11	10/11
ε =0.02	0	0.045	0.099	0.172	0.283	0.463	0.762	1.28	2.24	3.99	6.83
ε =0.04	0	0.091	0.020	0.345	0.568	0.927	1.53	2.57	4.47	7.94	1.36
ε =0.06	0	0.014	0.030	0.521	0.856	1.39	2.29	3.84	6.66	1.18	2.01
ε =0.08	0	0.018	0.040	0.701	1.15	1.87	3.05	5.10	8.79	1.55	2.63
ε =0.10	0	0.024	0.051	0.886	1.45	2.34	3.82	6.34	1.08	1.90	3.21

4.4 stress intensity factors for planar rectangular interfacial crack

The stress intensity factors (SIFs) are calculated for general aspect ratio with varying the polynomial exponents until $m=n$ =8. Table 3 shows the variations of SIFs along the crack front for a square interface crack a/b=1. It is seen that with varying ε from 0 to 0.1, the value of F_I decreases but the value of F_{II} increases. Table 4 shows the comparison between the results of square and disk shaped interfacial cracks. Here, the maximum values of F_I, F_{II} at $x=0$, $y=\pm b$ are indicated for the square crack. Under the same value of ε, the F_I value of a square interfacial crack is larger than that of disk shaped interfacial crack, while F_{II} of square interfacial crack is smaller than that of a disk shaped interfacial crack. Table 5 shows the values of F_I and F_{II} of a rectangular interfacial crack with varying the aspect ratio as a /b=1, 2, 4, 8. The F_I and F_{II} values of a rectangular interfacial crack are determined by ε alone [(20)]. The value of F_{III} is smaller and with the range $F_{I\max} \times 10^{-2}$.

Table 3(a) Dimensionless stress intensity factor F_I for a/b=1 at $y=b$

x/a	0/11	1/11	2/11	3/11	4/11	5/11	6/11	7/11	8/11	9/11	10/11
ε =0	0.7534	0.7516	0.7463	0.7373	0.7243	0.7063	0.6821	0.6500	0.6081	0.5513	0.4543
ε =0.02	0.7528	0.7511	0.7459	0.7369	0.7238	0.7058	0.6822	0.6514	0.6099	0.5490	0.4400
ε =0.04	0.7509	0.7492	0.7440	0.7351	0.7219	0.7040	0.6804	0.6495	0.6080	0.5470	0.4377
ε =0.06	0.7478	0.7461	0.7409	0.7320	0.7188	0.7009	0.6773	0.6464	0.6048	0.5436	0.4339
ε =0.08	0.7433	0.7416	0.7364	0.7275	0.7143	0.6965	0.6729	0.6419	0.6003	0.5389	0.4286
ε =0.10	0.7373	0.7356	0.7304	0.7215	0.7085	0.6906	0.6671	0.6362	0.5945	0.5329	0.4218

Table 3(b) Dimensionless stress intensity factor F_{II} for a/b=1 at $y=b$

x/a	0/11	1/11	2/11	3/11	4/11	5/11	6/11	7/11	8/11	9/11	10/11
ε =0.02	0.0274	0.0273	0.0272	0.0266	0.0260	0.0251	0.0239	0.0224	0.0204	0.0176	0.0134
ε =0.04	0.05417	0.0540	0.0535	0.0527	0.0514	0.0497	0.0474	0.0443	0.0403	0.0348	0.0365
ε =0.06	0.07985	0.0796	0.0789	0.0776	0.0758	0.0733	0.0699	0.0654	0.0595	0.0515	0.0393
ε =0.08	0.1040	0.1037	0.1028	0.1012	0.0988	0.0955	0.0911	0.0853	0.0776	0.0673	0.0515
ε =0.10	0.1263	0.1259	0.1248	0.1229	0.1201	0.1161	0.1107	0.1037	0.0945	0.0821	0.0629

Table 4 Comparison between the results of square and disk shaped interface cracks

ε	F_1		F_2	
	square	disk	square	disk
ε =0.02	0.7528	0.636	0.02738	0.030
ε =0.04	0.7509	0.636	0.05417	0.061
ε =0.06	0.7478	0.635	0.07985	0.091
ε =0.08	0.7433	0.634	0.1040	0.122
ε =0.10	0.7373	0.632	0.1263	0.152

Table5 Dimensionless stress intensity factor F_{I} and F_{II} at the point (0, b)

ε	F_{I}				F_{II}			
	a/b=1	a/b=2	a/b=4	a/b=8	a/b=1	a/b=2	a/b=4	a/b=8
ε =0.02	0.7528	0.9052	0.9760	0.9947	0.0274	0.0352	0.0388	0.0397
ε =0.04	0.7509	0.9038	0.9750	0.9938	0.0542	0.0696	0.0768	0.0786
ε =0.06	0.7478	0.9013	0.9730	0.9920	0.0798	0.1027	0.1134	0.1160
ε =0.08	0.7433	0.8975	0.9699	0.9891	0.1040	0.1338	0.1479	0.1515
ε =0.10	0.7373	0.8921	0.9654	0.9848	0.1263	0.1627	0.1801	0.1845

5. Conclusion

In this paper the stress intensity factors of a planar rectangular interfacial crack in three-dimensional bimaterials are studied through the singular integral equations on the basis of the body force method. The conclusion can be summarized as follows:

(1) The unknown functions were approximated by using fundamental densities and polynomials. Here the fundamental densities were chosen to express singular behavior of interface crack exactly.

(2) The present method provides smooth distributions of stress intensity factors along the crack front with good convergence. The remaining stresses along the crack surface are less than 10^{-5} when the polynomial exponents $m = n = 8$ (see Fig.3).

(3) The results for a/b=8 coincide with the 2D solutions to the three-digit in the range $|x/a| \le 0.5$ (see Table 3).

(4) The stress intensity factors of a rectangular interface crack were indicated accurately in Tables with varying the aspect ratio a/b and bimaterial constant ε (see Tables 3-5).

References

(1) Salganik, R.L., The Brittle Fracture of Cemented Bodies, *Prikladnaia metematica i mekhanika,* Vol. 27, (1963), pp. 957-962

(2) Erdogan, F., Stresses Distribution in a Non-homogeneous Elastic Plane with Crack, *Transaction of the ASME, Journal of Applied Mechanics,.,* Vol. 30, (1963), pp. 232-236

(3) England, A.H., A Crack between Dissimilar Media, *Transaction of the ASME, Journal of Applied Mechanics,* Vol. 32 , (1965), pp. 400-402

(4) Rice, J. R. and Sih, G. C. ,Plane Problems of Cracks in Dissimilar Media. *Transaction of the ASME, Journal of Applied Mechanics,* Vol. 32, (1965), pp. 418-423

(5) Comninou, M., The Interface Crack. *Transaction of the ASME, Journal of Applied Mechanics,* Vol. 44, (1977), pp.631-636

(6) Noda, N-A and Oda, K., Interaction Effect of Stress Intensity Factors for any Number of Collinear Interface Cracks, *International Journal of Fracture,* Vol. 84, (1997), pp.117-128

(7) Willis, J.R., Fracture Mechanics of Interfacial Crack, *Journal of the Mechanics and Physics of solids,* Vol. 19, (1971) ,pp.353-368

(8) Tucker, M. O., I n T wo-phase Solids under Longitudinal Shear Loading, *International Journal of Fracture,* Vol.10, (1974), pp. 323-336

(9) England, F. and Gupta,G.D., Bonded Wedges with an Interface Crack under Anti-plane Shear Loading, *International Journal of Fracture,* Vol.11, (1975), pp.593-593

(10) Willis, J.R., The Penny-Shaped Crack on an Interface, *J. Mech. Appl. Math.,* Vol. 25, (1972), pp.367-385

(11) Mossakovski, V. I., and Rybka, M. T., Generalization of the Griffith-senddon Criterion for the Case of a Non-homogeneous Body, *Prikl. Mat. Mekh.,* Vol. 28, (1964),

pp.1061-1069

(12) England, F., Stress Distribution in Bonded Dissimilar Materials Containing Circular or Ring-Shaped Cavities, *Trans. ASME, Ser. E, J. Appl. Mech.*, Vol. 32, (1965), pp.829-836

(13) Kassir, M. K., and Bregman, A M., The Stress Intensity Factor for a Penny-Shaped Crack between Two Dissimilar Materials, *Trans. ASME. Ser. E. J. Appl. Mech.*,Vol. 39, (1972), pp.308-310

(14) Lowengrub, M. and Senddon,I. N., The Effect of Internal Pressure on a Penny-Shaped Crack at the Interface of Two Bonded Dissimilar Elastic Half-Spaces, *Int. J. Engng. Sci.*, Vol. 12, (1974), pp.387-396

(15) (15) Keer, L. M. Chen, S. H. and Comninou,M., The Interface Penny-Shaped Crack Reconsidered, *Int, J. Engng Sci.*, Vol.16, (1978), pp. 765-772

(16) Shibuya, T., Stress Analysis of the Vicinity of an Elliptical Crack at the Interface of Two Bonded Half-Spaces, *JSME Int. J.*, Vol.32, (1989), pp.485-491

(17) Yuuki, R., Cao, X. F., Boundary Element Analysis to Stress Intensity Factor of Interface Crack, *Tran. of JSME* (in Japanese) No.55-510,(1989), pp.340-347

(18) Takakuda, K., Shibuya, T., and Coizumi, T.,. Stress Analysis to Interface Crack in Bonded Semi-Infinite Plate, *Tran. of JSME* (in Japanese) No. 780-3, (1978), pp.167-169

(19) Noda, N. A., Kagita M., and Chen, M, C., Analysis of Stress Intensity Factors of a Ring-Shaped Interface Crack, *International Journal of Solids and Structures*, Vol.40, No.24, (2003), pp.6577-6592

(20) Noda, N.A., Xu, C. H., and Takase, Y., Stress Intensity Factor for a Planar Interfacial Crack in Three Dimensional Bimaterials, *Transaction of the Japan Society of Mechanical Engineering, Series A*（in Japanese, submitted)

(21) Chen M. C. Noda, N. A. and Tang, R. J.,, Application of Finite-part Integrals to Planar Interfacial Fracture Problems in Three Dimensional Bimaterials, *Journal of Applied Mechanics,* Vol.66, (1999), pp.885-890

(22) Qin T.Y. and Noda, N.A., Stress Intensity Factors of Rectangular Crack Meeting a Bimateral Interface, *International Journal of Solids and Structures,* Vol. 40,(2003), pp.2473-2486

(23) Wang, Q., Noda, N.A. and Honda, M., Chen, M.C., Variation of Stress Intensity Factors along the Front of 3D Rectangular Crack by Using a Singular Integral Equation Method, *International Journal of Fracture*, Vol.108, (2001),pp.119-131

(24) Noda, N.A. and Miyoshi, S., Variation of Stress Intensity Factor and Crack Opening Displacement of Semi-Elliptical Surface Crack, *International Journal of Fracture*, Vol.75, (1996),pp.19-48